ANALYSIS OF REINFORCED CONCRETE SLAB PUNCHING

By

D. DALMY

Department of Reinforced Concrete Structures,
Technical University, Budapest

(Received September 20, 1977)

Presented by Prof. Dr. Árpád OROSZ

1. Introduction

The stress peak at the vicinity of point loads acting on reinforced concrete slabs may cause local failure by punching. The flat slabs are widely applied in construction. In this type of structures the slab-column junctions are rigid, moment-bearing, thus the column reactions are paralleled by moments; the column reactions are eccentric.

Tests have been made at the Department of Reinforced Concrete Structures to determine ultimate load at punching and test results have been applied to establish a theory on punching.

The theoretical analysis is based on the upper bound theorem of plasticity. The theoretical approach involves the compressive membrane effect.

Deductions may be of use for determining the central and eccentric ultimate punching load of reinforced concrete slabs.

2. Historical survey

As early as soon after the advent of reinforced concrete structures, designing and research engineers recognized the importance of punching analyses. In the early 1900's, tests on this phenomenon [1] suggested to determine the ultimate punching load from the shear strength of the punching cone surface, a method still underlying standard specifications in several countries.

Subsequent test [2] hinted to the importance of flexural strength of the slab around the column for the occurrence of punching.

In spite of the intensive research and testing program of the past two decades, there is no unambiguous solution for safely predicting the punching load.

Methods suggested for determining the punching load belong to two groups:

a) semi-empirical relationships based on great many test results [3];

b) idealized models constructed on the basis of test observations [4].

In connection with methods suggested for punching analyses, the following statements hold:

1. Experimentally determined constants of empirical or semi-empirical relationships cannot be directly adopted because of heterogeneous standard specifications on strength of materials and safety.

2. Relationships deduced from idealized models are extremely complex, inexpedient and often contradictory.

3. Methods for determining the ultimate load at punching are only adequate for forces without unbalanced moment, eccentric punching force relationships are too rough approximations [3].

4. There is no relationship to take the compressive membrane effect superposed to the ultimate punching load in slabs with lateral restraint into consideration.

3. Tests to determine the ultimate punching load

Tests to determine the ultimate punching load have been made on structural members made of the same material i.e. reinforced concrete ([5], [6], [7]) such as:

— uniformly loaded, square r.c. slabs supported on four colums,

— circular slabs under central or eccentric load.

The r.c. flat slabs with top and bottom fabric reinforcement failed in punching as a rule. Typical failure pattern of a flat slab on the load side is seen in Fig. 1. The mesh drawn on the slab has 10 by 10 cm divisions.

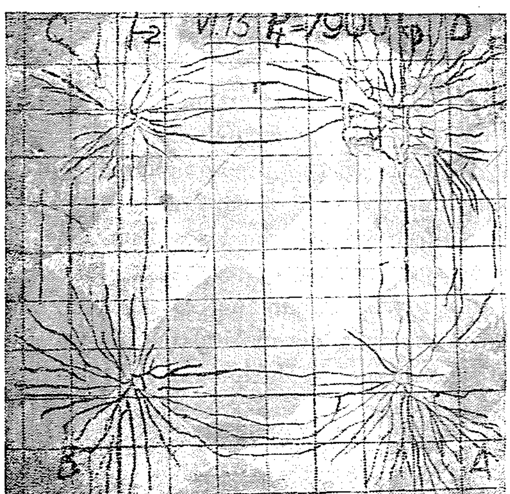

Fig. 1

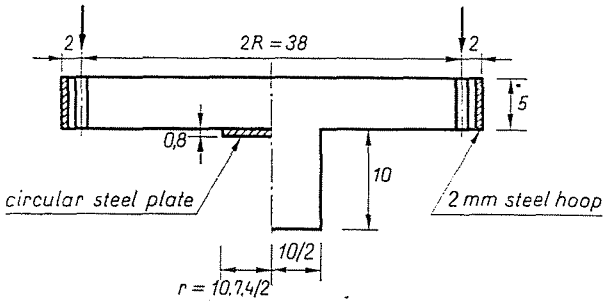

Fig. 2

Circular slab tests involved the effects of
— column diameter,
— load eccentricity,
— moment bearing
on the ultimate punching load of the slab.

Test specimens are seen in Fig. 2. Those in the left side have been designed for testing the effect of column diameter, and those in the right side serve for eccentric load tests.

Circular slab specimens have been cast in a stiff steel hoop as seen in Fig. 2, replacing slab parts omitted from the column-to-slab connection region.

Strain gauges on the steel hoop checked the compressive membrane effect under load.

Test arrangement is seen in Fig. 3.

The typical failure pattern of a circular slab specimen is seen in Fig. 4.

Test results and observation have led to the following conclusions:

1. *Flat slab tests*:

a) In general, slabs failed in punching, the punching cone size little changed as a function of the reinforcement percentage.

b) Test load-deflection diagrams showed that the moment-bearing capacity of slabs increased by compressive membrane effect was not exhausted at the moment of failure by punching.

2. *Circular slab tests*:

a) Column diameter much affects the features and the ultimate load at punching. In case of a small column size, no regular punching cone, present in usual tests, develops, the concrete exhibits intensive crushing in the capital region.

b) The arching effect due to the lateral restraint of slabs much adds to the ultimate load at punching: 60% difference was found between test results and ultimate loads according to the yield line theory.

c) Circular column section is optimum for ultimate load bearing.

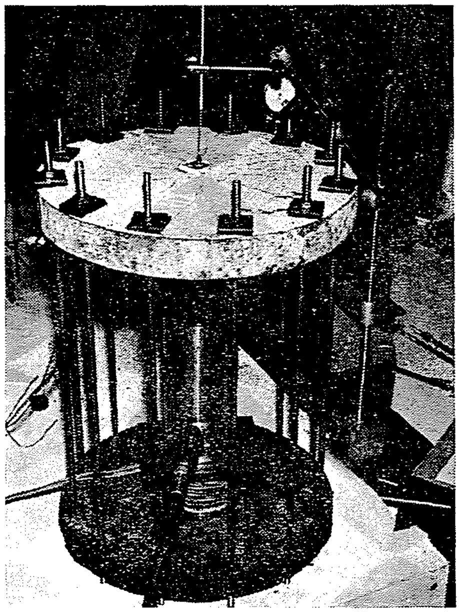

Fig. 3

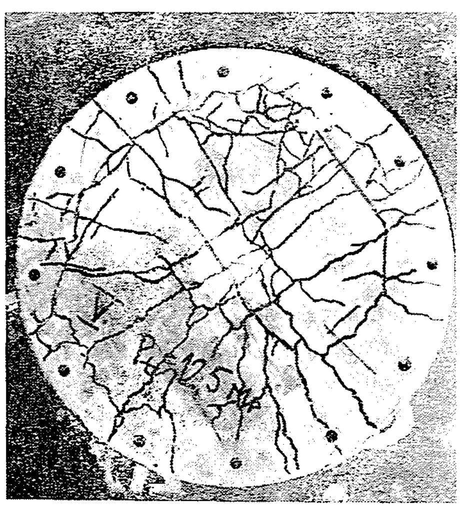

Fig. 4

d) In case of an eccentric punching load, the ultimate load at punching is reduced by the eccentricity of the applied load. Test results have been plotted in Fig. 5 as ultimate punching load P vs. unbalanced moment determined from the eccentricity of the ultimate punching load.

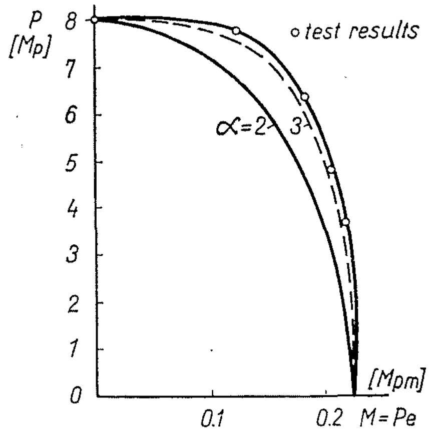

Fig. 5

4. Theoretical analysis of the ultimate punching load

Our theoretical analyses of punching started from test results and observations.

Ultimate punching load has also been determined for an eccentric punching load, taking the compressive membrane effect into consideration. Analyses referred to the case of regular punching cone.

4.1. *Assumptions of the theoretical analysis*

Test results and observations induced us to involve the following aspects in the theoretical deductions for the complex analysis of the punching phenomenon:

1. Determination of the ultimate punching load at the inner columns of flat slabs can take the arching effect into consideration.

2. A simplified model shown in Fig. 6, typical of the punching phenomenon, has been developed to take the arching effect into consideration. The ulti-

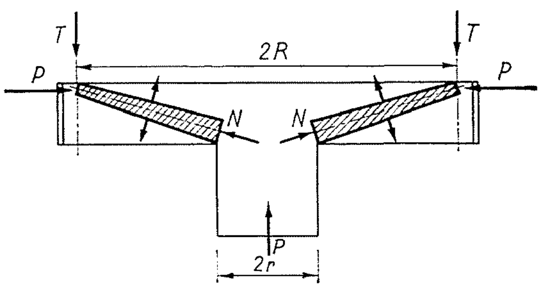

Fig. 6

mate punching load is where the tensile strain — perpendicular to the generatrice of the punching cone — reaches the ultimate concrete elongation.

3. In case of an eccentric punching force it is sufficient to establish two characteristic points in Fig. 5 — intersection points of the curve with the co-ordinate axes —, relating to the case of axial load and only bending moment on the column. Other assumptions in our theoretical analysis were the same as those usual for the yield line theory:

1. the materials (steel and concrete) are rigid-perfectly plastic;
2. the original yield line pattern does not change during deformation.

4.2. *Fundamentals of the theoretical analysis*

Several theoretical proofs have been published [8, 9, 10] on the load capacity increase due to arching effect in r.c. slabs with edges restrained against horizontal displacement. Theoretical analyses applied the upper bound theorem of plasticity.

For a yield line in the failure mechanism acted upon by moment M and normal force N, the rate of energy dissipation along its elementary length $\mathrm{d}t$ is:

$$\mathrm{d}D = \dot{\varkappa}(M + z_0 N)\,\mathrm{d}t$$

where: $\dot{\varkappa}$ = rotation rate of cross section

z_0 = spacing between the neutral axis and the origin of the co-ordinate axis.

[10] stated the general relationship for the energy dissipation along the elementary yield line length to be for reinforced concrete sections:

$$\mathrm{d}D = \dot{\varkappa}\left[M_0 \frac{1+\xi^2}{2} + \xi \operatorname{sgn} \dot{\varkappa} + 2\mu_i(\xi - \xi_i)\right]\mathrm{d}t \quad \text{if } \xi \leq 1$$

where:

$\xi = z_0/0.5$ h

h = effective depth of the cross section

$M_0 = \dfrac{\sigma_c h^2}{4}$

$\mu_i = \dfrac{\sigma_s F_{si}}{\sigma_c h}$ specific steel percentage in row i.

The energy dissipation extended to the entire yield line pattern equals the external work ($D = T$) where the dissipation rate is at its minimum:

$$\frac{\mathrm{d}D}{\mathrm{d}\xi} = 0\,.$$

This relationship has been applied to determine the ultimate punching load [11] in case of

a) axial load;

b) column bearing only a moment.

4.3. *Ultimate axial punching load*

Let the circular slab of radius R, restrained along its edge, be loaded by an axial load P on the column stub of radius r. Failure mechanism is seen in Fig. 7.

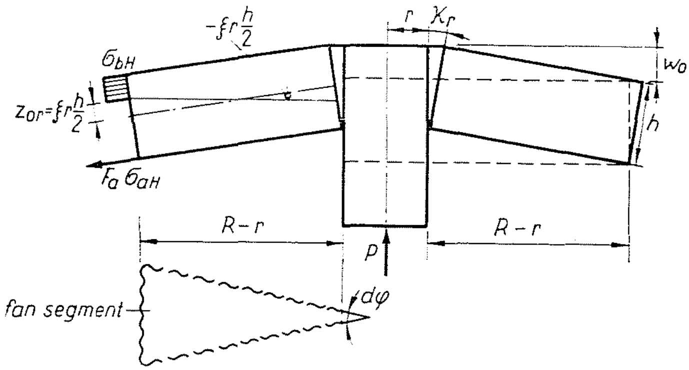

Fig. 7

Relative depths ξ_r and ξ_φ are clearly seen to be connected by a geometrical relationship.

Applying the relationship in item 4.2 on a circular ring segment with an elementary $d\varphi$, let us consider the case of identity between top and bottom reinforcements of the circular slab $\mu_t = \mu_b = \mu$.

Energy dissipation rate of the elementary circular ring segment becomes after minimizing:

$$D = M_0 \dot{\varkappa} R \mathrm{d}\varphi \left(1 + 8\mu - \alpha\beta + \frac{5}{12}\alpha^2\beta^2\right).$$

Finally, the external work equals the energy dissipation calculated for the entire circular slab

$$P w_0 = \int_0^{2\pi} D \mathrm{d}\varphi$$

yielding for the axial ultimate punching load:

$$P_u = M_0 \beta 2\pi \left(1 + 8\mu - \alpha\beta + \frac{5}{12}\alpha^2\beta^2\right).$$

4.4. *Punching due to a single bending moment on the column*

Punching in case of an unbalanced moment will be analysed on the structural model seen in Fig. 8.

The vertical deflection e at any point of the circumference of the column and the maximum deflection Δ in the bending moment plane are related by:

$$e = \Delta \sin \varphi .$$

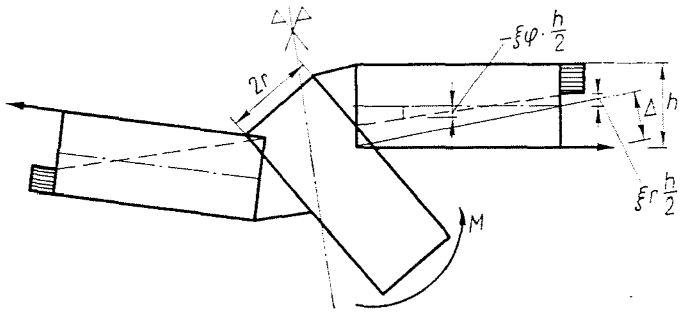

Fig. 8

Relationships and assumptions in items 4.2 and 4.3 will be involved in the energy dissipation relationship for a circular ring segment slab of elementary central angle $d\varphi$:

$$D = M_0 \frac{\Delta \sin \varphi}{R - r} R \, d\varphi \left(1 + 8\mu - \frac{2\Delta \sin \varphi}{h} + \frac{5}{12} \frac{\Delta^2 \sin^2 \varphi}{h^2} \beta^2\right) .$$

Equalizing the external work of the moment acting on the column to the energy dissipation determined for the entire circular slab:

$$M_u = \frac{\Delta}{r} = 4 \int_0^{\pi/2} D d\varphi$$

yields the moment:

$$M_u = M_0 r \beta \left(1 + 8\mu - \frac{\Delta \pi}{2h} + \frac{5}{18} \frac{\Delta^2}{h2} \beta^2\right) .$$

4.5 *Determination of the failure in punching*

Relationships in items 4.3 and 4.4. yield the punching column force or moment as a function of the column deflection. Experimental observations in item 4.1 permit to determine the maximum column deflection at failure.

Starting from the structural model in Fig. 6, for the sake of simplicity the median surface of the truncated cone is assumed to be diagonal to the circular ring segments of the yield pattern (see line A—C in Fig. 9).

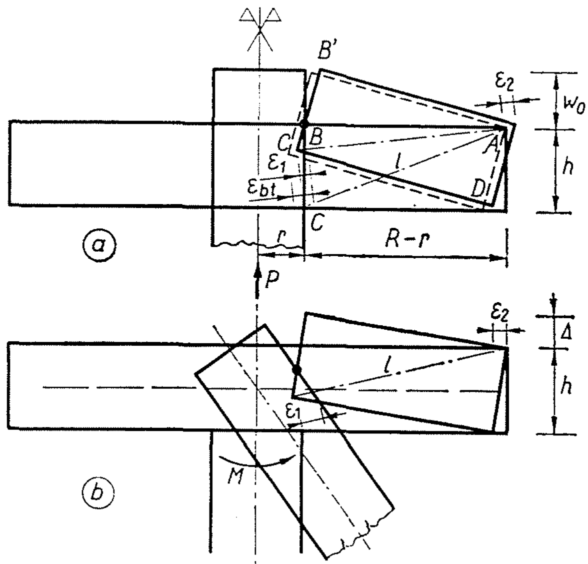

Fig. 9

Experimental observations permit the assumption of identity between modes of failure of the truncated cone and the concrete prisms in compression, hence it is sufficient to determine the maximum column deflection (w_0 or Δ) accompanied by the maximum ultimate compression ε_c in the circular ring segment diagonal, typical of the concrete. Consideration of Fig. 9 permits to write a simple geometrical relationship between column deflection and ultimate compressive strain.

Omitting derivations, the maximum column deflection under an axial load becomes:

$$w_0 = \frac{(R-r)^2}{h} \frac{\varepsilon_c}{1-\varepsilon_c} \, .$$

The maximum column deflection under a moment is given by:

$$h\Delta^2 + \Delta[(R-r)^2 + h(R-r)(1-\varepsilon_c)] - (R-r)^3\varepsilon_c = 0 \, .$$

5. Numerical example

To check the theoretical solution, ultimate punching load of the flat slab on four supports described in item 3 (Fig. 1) has been computed, with the following data:

Material characteristics:
- concrete strength $\sigma_c = 400$ kp/cm^2
- ultimate concrete compressive strain $\varepsilon_c = 3.3^0/_{00}$
- reinforcing steel $\varnothing$ 3/5.9 cm, bottom and top steel fabric
- yield strength of steel $\sigma_s = 3100$ kp/cm^2.

Ultimate test load:
Column reaction entraining punching (mean ultimate load of two slabs of identical design)

$$P_u^{\text{exp}} = 1800 \text{ kp}.$$

Ultimate punching load has been determined as described in item 4.3.

1. Auxiliary design magnitudes:
   - Radius of the substituting circular column:

$$r = \frac{4a}{2\pi}; \qquad r = 3.8 \text{ cm}$$

   - Specific steel percentage:

$$\mu = \frac{F_s, \sigma_s}{\sigma_c \cdot h} = 0.072$$

   - Cross sectional moment:

$$M_0 = \frac{\sigma_c \cdot h^2}{4} = 170 \text{ kpcm/cm}$$

   - Radius of the punching cone has been determined according to [12] as $R = 16.5$ cm (15 cm in the test)

$$R = \sqrt[3]{\frac{P_c}{P}}$$

   - The relative radius:

$$\beta = \frac{R}{R - r} = 1.3$$

   - Maximum column deflection according to item 4.5:

$$w_0 - \frac{(R - r)^2}{h} \cdot \frac{\varepsilon_c}{1 - \varepsilon_c} = 4.2 \text{ mm (5 mm in the test)}$$

   - Relative deflection:

$$\alpha = \frac{w_0}{h} = 0.32\,.$$

2. Ultimate punching load according to item 4.3, substituting the previously obtained auxiliary magnitudes:

$$P_u^{\text{theor}} = 1690 \text{ kp} < P_u^{\text{exp}} = 1800 \text{ kp}\,.$$

Calculated and experimentally obtained ultimate loads differ by less than 10%.

6. Conclusions

The presented numerical example shows the consideration of the compressive membrane effect to yield a fair value for the ultimate punching load.

For an eccentric punching force, it is sufficient to determine two typical limiting cases: those of axial P_{0u} and of the ultimate punching load of infinite eccentricity M_{0u}. In any intermediate case, the eccentric ultimate punching load can be checked by the interaction curve in Fig. 5; e.g. using an exponent $\alpha = 2$ yields a simple, easy relationship for analysing or checking the eccentric ultimate punching load:

$$\left(\frac{M}{M_{0u}}\right)^2 + \left(\frac{P}{P_{0u}}\right)^2 \leqq 1 .$$

That is, having determined M_{0u} and P_{0u} depending on the r.c. slab permits to check the maximum eccentricity of the ultimate punching load.

Summary

Punching tests as well as the method of analysis of punching under axial and eccentric ultimate punching loads based on test results have been described. The theoretical analysis is based on the yield line theory, taking also the compressive membrane effect in the slab into consideration.

References

1. TALBOT: Reinforced Concrete Wall Footings and Column Footings, Bull. of Univ. of Illinois No. 67, 1915.
2. ELSTNER, HOGNESTAD: An Investigation of Reinforced Concrete Flat Slabs. Journal of ACI 1957.
3. MOE, J.: Shearing Strength of Reinforced Concrete Slabs. P.C.A.Research and Development Laboratories Bull. D. 47.
4. KINNUNEN, NYLANDER: Punching of Concrete Slabs Without Shear Reinforcement. Trans. of Royal Inst. of Techn. Stockholm, 1960.
5. Model tests on slabs on supports.* (Report, Department of Reinforced Concrete Structures, Technical University, Budapest, commissioned by IPARTERV, 1968, 1969.)
6. Model test on the Baross tér pedestrian subway;* (Report, Department of Reinforced Concrete Structures, Technical University, Budapest, commissioned by FÖMTERV, 1968.)
7. Experimental analysis of the punching of r.c. slabs;* (Report, Department of Reinforced Concrete Structures, Technical University, Budapest, Commissioned by IPARTERV 1971.)
8. WOOD, R. H.: Plastic and Elastic Design of Slabs and Plates. Thames and Hudson, London 1961.
9. JANAS, M., SAWCZUK, A.: Influence of Position of Lateral Restraint on Carrying Capacities of Plates. Arch. Inz. Lad. Tom. XII. — Z3/1966.
10. JANAS, M.: Large Plastic Deformation of Reinforced Concrete Slabs. Int. J. Solid Structures 1968. Vol. 4. pp. 61—74.
11. DALMY, D.: Punching of r.c. slabs.* (Doctor's Thesis 1972).
12. KALISZKY, S.: Plastic design of r.c. slabs.* Műszaki Könyvkiadó 1967.

Dr. Dénes DALMY, H-1521, Budapest

* In Hungarian